

MICROSCOPIC DESCRIPTION OF THE LIQUID-GAS COEXISTENCE CURVE FOR MORSE FLUIDS IN THE IMMEDIATE VICINITY OF THE CRITICAL POINT

I.V. PYLYUK, M.P. KOZLOVSKII, R.V. ROMANIK¹

Institute for Condensed Matter Physics of the National Academy of Sciences of Ukraine, 1 Svientsitskii Str., 79011 Lviv, Ukraine

The present work is aimed at investigating the behavior of Morse fluids in the immediate vicinity of the critical point within the framework of a cell model. This region is of both fundamental and practical importance, yet presents analytical challenges due to the significant influence of order parameter fluctuations. An analytical procedure is developed to construct the upper part of the liquid-gas coexistence curve and calculate its diameter, incorporating the non-Gaussian (quartic) distribution of fluctuations. An explicit expression is derived for the temperature-dependent analytical term appearing in the expression for the rectilinear diameter. The numerical evaluation of the relevant quantities is carried out using Morse potential parameters representative of sodium. The coexistence curve is constructed both with and without the inclusion of the analytical temperature-dependent term in the calculation. A specific condition is identified under which the agreement between the presented binodal branches and Monte Carlo simulation data from other study, extrapolated to the immediate vicinity of the critical point, is improved. It is shown that better agreement is achieved when the analytical term is included in the calculation of the liquid branch and omitted in the gas branch. The proposed analytical approach may provide useful insight for the theoretical study of critical phenomena in more complex fluid systems.

PACS numbers: 05.70.Ce, 64.60.F-, 64.70.F-

Keywords: grand partition function, Morse potential, critical point, coexistence curve, rectilinear diameter

1 Introduction

Our calculations within the framework of the grand canonical ensemble are performed in the immediate vicinity of the critical point, which is a problematic area for theoretical and experimental studies. The region in the vicinity

¹e-mail: romanik@icmp.lviv.ua

of the critical point is of both fundamental and applied interest, yet remains difficult to analyze due to the significant role of fluctuation effects. Calculations in this region are challenging to carry out (see, for example, Refs. [1, 2], where computer simulation data for the upper parts of the coexistence curves in the temperature-density plane are lacking in the immediate vicinity of the critical point). The high critical temperatures characteristic of many metals still cannot be reached experimentally [3].

This paper continues the previous studies [4–7], based on a cell fluid model with the Morse interaction potential. An analytical method has been developed to describe the upper part of the liquid-gas coexistence curve (i.e., the top of the coexistence dome) for Morse fluids, taking into account the non-Gaussian (quartic) distribution of order parameter fluctuations. The order parameter and the coexistence curve diameter, both playing an important role in the study of phase transitions, have been calculated.

The presence of a singularity in the coexistence curve diameter has been theoretically predicted (see, for example, Refs. [8–10]). However, the experimental observation of this effect is complicated by the fact that the singular term may be masked by other contributions of comparable magnitudes and similar exponents [11]. Since the exponent of the relative temperature in the singular term is close to unity, the true singularity is difficult to distinguish from the analytical contribution. This anomaly in the diameter appears just below the critical point and is challenging to capture in molecular simulations [1]. In their molecular dynamics study, the authors of Ref. [1] applied the equation corresponding to the law of the rectilinear diameter. The behavior of coexistence curve diameters in fluids remains an active topic of current research (see, for example, Refs. [12–14]).

In the present study, analytical expressions necessary for constructing the top of the liquid-gas coexistence curve and for analyzing its diameter have been obtained. The numerical values of the relevant quantities are provided.

2 Basic expressions

The theoretical description of the critical behavior of a simple fluid is carried out within the framework of a cell model. We consider an open system of classical interacting particles contained within a volume V . This volume is divided into N_v cells, each of volume $v = V/N_v = c^3$, where c denotes the linear size of a cell. In contrast to the cell gas model described in [15, 16],

where each cell is assumed to contain at most one particle or to be empty, our approach allows a cell to contain multiple particles.

In terms of the collective variables $\rho_{\mathbf{k}}$, the expression for the grand partition function of the cell fluid model in the approximation of the simplest non-Gaussian quartic fluctuation distribution (the ρ^4 model) can be written as [4, 5, 17]

$$\Xi = g_W e^{N_v(E_\mu - a_0)} \int (d\rho)^{N_v} \exp \left[M N_v^{1/2} \rho_0 - \frac{1}{2} \sum_{\mathbf{k} \in \mathcal{B}} d(k) \rho_{\mathbf{k}} \rho_{-\mathbf{k}} - \frac{a_4}{4!} N_v^{-1} \sum_{\substack{\mathbf{k}_1, \dots, \mathbf{k}_4 \\ \mathbf{k}_i \in \mathcal{B}}} \rho_{\mathbf{k}_1} \cdots \rho_{\mathbf{k}_4} \delta_{\mathbf{k}_1 + \dots + \mathbf{k}_4} \right]. \quad (1)$$

Here

$$\begin{aligned} g_W &= \prod_{\mathbf{k} \in \mathcal{B}} (2\pi\beta W(k))^{-1/2}, \\ E_\mu &= -\frac{\beta W(0)}{2} (M + \tilde{a}_1)^2 + M a_{34} + \frac{1}{2} d(0) a_{34}^2 - \frac{a_4}{24} a_{34}^4, \\ a_{34} &= -a_3/a_4, \\ M &= \mu/W(0) - \tilde{a}_1, \quad \tilde{a}_1 = a_1 + d(0) a_{34} + \frac{a_4}{6} a_{34}^3, \\ d(k) &= \frac{1}{\beta W(k)} - \tilde{a}_2, \quad \tilde{a}_2 = \frac{a_4}{2} a_{34}^2 - a_2, \end{aligned} \quad (2)$$

and $\delta_{\mathbf{k}_1 + \dots + \mathbf{k}_4}$ is the Kronecker symbol. The wave vector \mathbf{k} belongs to the set

$$\mathcal{B} = \left\{ \mathbf{k} = (k_1, k_2, k_3) \left| k_i = -\frac{\pi}{c} + \frac{2\pi}{c} \frac{n_i}{N_a}; n_i = 1, 2, \dots, N_a; i = 1, 2, 3; N_v = N_a^3 \right. \right\},$$

where N_a is the number of cells along each axis. The quantity M , linearly related to the thermodynamic chemical potential μ , will hereafter be treated as the chemical potential. Above, $\beta = 1/(k_B T)$ is the inverse temperature, k_B is the Boltzmann constant, and T is the temperature. The Fourier transform of the effective interaction potential $W(k)$ includes the Fourier transforms of the attractive and repulsive parts of the Morse potential, which is defined as

$$\tilde{U}_{l_{12}} = \Psi_{l_{12}} - U_{l_{12}}; \quad \Psi_{l_{12}} = D e^{-2(l_{12}-1)/\alpha_R}, \quad U_{l_{12}} = 2D e^{-(l_{12}-1)/\alpha_R}. \quad (3)$$

Here $\alpha_R = \alpha/R_0$, and α is the effective interaction radius. The parameter R_0 corresponds to the minimum of the function $\tilde{U}_{l_{12}}$, and D determines the

depth of a potential well. The Morse potential $\tilde{U}_{l_{12}}$ is a function of the distance $l_{12} = |\mathbf{l}_1 - \mathbf{l}_2|$ between cells \mathbf{l}_1 and \mathbf{l}_2 . For convenience, all lengths are measured in R_0 -units. As a result, R_0 - and R_0^3 -units are used for the linear size of each cell c and volume v , respectively.

The coefficients [5, 17]

$$\begin{aligned} a_0(T) &= -\ln T_0(v, p(T)), \quad a_1(T) = -\frac{T_1(v, p(T))}{T_0(v, p(T))}, \\ a_2(T) &= -\frac{T_2(v, p(T))}{T_0(v, p(T))} + a_1^2(T), \\ a_3(T) &= -\frac{T_3(v, p(T))}{T_0(v, p(T))} - a_1^3(T) + 3a_1(T)a_2(T), \\ a_4(T) &= -\frac{T_4(v, p(T))}{T_0(v, p(T))} + a_1^4(T) - 6a_1^2(T)a_2(T) + 4a_1(T)a_3(T) + 3a_2^2(T) \end{aligned} \quad (4)$$

appearing in the expression (1) for Ξ are presented in terms of special functions

$$T_n(v, p(T)) = \sum_{m=0}^{\infty} \frac{v^m}{m!} m^n e^{-p(T)m^2}, \quad (5)$$

which are rapidly convergent series due to the condition $p(T) > 0$. The parameter

$$p(T) = \frac{1}{2}\beta\chi\Psi(0), \quad (6)$$

is proportional to the Fourier transform $\Psi(0) = D\pi\alpha_R^3 e^{2R_0/\alpha}/v$ of the repulsive part of the interaction potential at $k = 0$ [4, 5, 17]. The positive parameter χ forms the Jacobian of transition from individual coordinates to collective variables. Thus, the quantities $a_n(T)$ are functions of temperature and microscopic parameters of the interaction potential, in particular, of the ratio R_0/α characterizing real substances [2, 18]. Further, for convenience, we will denote these quantities $a_n(T)$ as a_n .

Having the final formula for the logarithm of the grand partition function [4, 5], we can find the average number of particles

$$\bar{N} = \frac{\partial \ln \Xi}{\partial \beta \mu}. \quad (7)$$

This relation allows us to express the chemical potential in terms of the

average number of particles \bar{N} or in terms of the average density

$$\bar{n} = \frac{\bar{N}}{N_v} = \left(\frac{\bar{N}}{V} \right) v, \quad (8)$$

where v is the volume of a cubic cell.

3 Relationship between the density and the chemical potential of fluid

The nonlinear equation, which describes the relationship between the density \bar{n} and the chemical potential M , can be represented as [5, 19]

$$\bar{n} = n_g - M + \sigma_{00}^{(-)} \left(\tilde{h}^2 + h_{cm}^2 \right)^{\frac{d-2}{2(d+2)}}. \quad (9)$$

Here $d = 3$ is the space dimension. The quantity

$$\tilde{h} = M(\beta W(0))^{1/2} \quad (10)$$

is proportional to the chemical potential. The quantity

$$h_{cm} = \tilde{\tau}_1^{\ln E_1 / \ln E_2} \quad (11)$$

is characterized by the renormalized relative temperature

$$\tilde{\tau}_1 = -\tau \frac{c_{11}}{q} E_2^{n_0}, \quad (12)$$

where $\tau = (T - T_c)/T_c$ (T_c is the critical temperature), and E_l are eigenvalues of the renormalization group linear transformation matrix. The quantity c_{11} characterizes one of the coefficients in the solutions of recurrence relations for the ρ^4 model, n_0 is the difference between the points of the exit of the system from the critical fluctuation regime at $T > T_c$ and $T < T_c$, and q is associated with the averaging of the wave vector square. Additional information about these parameters can be found in Refs. [4, 5]. The term

$$n_g = -a_1 - a_2 a_{34} + \frac{a_4}{3} a_{34}^3 \quad (13)$$

appearing in Eq. (9) is determined by the coefficients a_n , which are given in Eqs. (4) and are included in the initial expression (1) for the grand partition

function. The coefficient $\sigma_{00}^{(-)}$ in Eq. (9) is a function of the quantity $\alpha_m = \tilde{h}/h_{cm}$, which includes the chemical potential M and the relative temperature τ (see Ref. [5]).

In this paper, the expression (9) for \bar{n} at $M = -0$ and $M = +0$ will be used to derive the equations describing the liquid-gas coexistence curve in the temperature-density plane. Based on these equations, we will obtain explicit analytical expressions for the order parameter of the system and the diameter of the coexistence curve. Let us start the calculations.

Using the relation $\beta = \beta_c(1+\tau)^{-1}$ and singling out temperature explicitly in Eq. (6), we arrive at the following expression accurate to within $\tau \ll 1$:

$$p(T) = p_0(1 - \tau). \quad (14)$$

Here $p_0 = \beta_c \chi \Psi(0)/2$. Substituting expression (14) for $p(T)$ into Eq. (5), and retaining terms within the linear approximation in τ , leads to the following relation

$$T_n(v, p(T)) = T_n(v, p_0) + T_{n+2}(v, p_0)p_0\tau. \quad (15)$$

Taking into account Eq. (15) and introducing the notations

$$T_n(v, p_0) \equiv T_n, \quad \frac{T_m(v, p_0)}{T_n(v, p_0)} \equiv T_{mn}, \quad (16)$$

we obtain the following expressions for the coefficients a_n [see Eqs. (4)]:

$$\begin{aligned} a_0 &= a_{0c} + a_0^{(1)}\tau, & a_1 &= a_{1c} + a_1^{(1)}\tau, & a_2 &= a_{2c} + a_2^{(1)}\tau, \\ a_3 &= a_{3c} + a_3^{(1)}\tau, & a_4 &= a_{4c} + a_4^{(1)}\tau. \end{aligned} \quad (17)$$

Here

$$\begin{aligned} a_{0c} &= -\ln T_0, & a_0^{(1)} &= -T_{20}p_0, \\ a_{1c} &= -T_{10}, & a_1^{(1)} &= a_{1c}(-T_{20} + T_{31})p_0, \\ a_{2c} &= -T_{20} + a_{1c}^2, & a_2^{(1)} &= 2a_{1c}a_1^{(1)} + (T_{20} - T_{42})T_{20}p_0, \\ a_{3c} &= -T_{30} - a_{1c}^3 + 3a_{1c}a_{2c}, \\ a_3^{(1)} &= 3(a_{1c}^2a_1^{(1)} + a_{1c}a_2^{(1)} + a_1^{(1)}a_{2c}) + (T_{20} - T_{53})T_{30}p_0, \\ a_{4c} &= -T_{40} + a_{1c}^4 - 6a_{1c}^2a_{2c} + 4a_{1c}a_{3c} + 3a_{2c}^2, \\ a_4^{(1)} &= 4a_{1c}^3a_1^{(1)} - 6(a_{1c}^2a_2^{(1)} + 2a_{1c}a_1^{(1)}a_{2c}) + 4(a_{1c}a_3^{(1)} + a_1^{(1)}a_{3c}) \\ &\quad + 6a_{2c}a_2^{(1)} + (T_{20} - T_{64})T_{40}p_0. \end{aligned} \quad (18)$$

According to Eq. (13), the explicit dependence of the quantity n_g on the relative temperature τ can be obtained using Eqs. (17) as well as the relation

$$a_{34} = a_{34c} + a_{34}^{(1)}\tau, \quad (19)$$

where

$$a_{34c} = -\frac{a_{3c}}{a_{4c}}, \quad a_{34}^{(1)} = a_{34c} \left(\frac{a_3^{(1)}}{a_{3c}} - \frac{a_4^{(1)}}{a_{4c}} \right). \quad (20)$$

We arrive at the expression

$$n_g = n_{gc} + n_g^{(1)}\tau. \quad (21)$$

Here

$$\begin{aligned} n_{gc} &= -a_{1c} - a_{2c}a_{34c} + \frac{a_{4c}}{3}a_{34c}^3, \\ n_g^{(1)} &= -a_1^{(1)} - a_{2c}a_{34}^{(1)} - a_2^{(1)}a_{34c} + \frac{1}{3} \left(3a_{4c}a_{34c}^2a_{34}^{(1)} + a_{34c}^3a_4^{(1)} \right). \end{aligned} \quad (22)$$

The components of the quantities a_n , a_{34} , and n_g are given in Tables 1, 2, and 3 for the set of parameters $R_0/\alpha = 2.9544$ (which is typical of sodium (Na), see Refs. [2, 18]) and $\chi = 1.1243$, $p_0 = 1.8100$, $v = 2.4191$ (see Refs. [4, 5, 17]).

As is seen from Table 3, the quantities $\sigma_{030}'^{(-)}$ and $\sigma_{010}'^{(+)}$, as well as $\sigma_{00c}^{(-)}$ ($\sigma_{030}'^{(-)}$)

Table 1: Values of the quantities determining the coefficients a_0 , a_1 , and a_2 .

a_{0c}	$a_0^{(1)}$	a_{1c}	$a_1^{(1)}$	a_{2c}	$a_2^{(1)}$
-0.3350	-0.5234	-0.2862	-0.3845	-0.2073	-0.1846

Table 2: Numerical estimates of the quantities determining the coefficients a_3 , a_4 , and a_{34} .

a_{3c}	$a_3^{(1)}$	a_{4c}	$a_4^{(1)}$	a_{34c}	$a_{34}^{(1)}$
-0.0938	-0.1419	0.0376	0.4110	2.4925	-23.4516

and $\sigma_{00c}^{(-)}$ ($\sigma_{010}'^{(+)}$), have equal magnitudes but opposite signs. This property will be used in Section 5 in the manipulations involving Eqs. (30) and (31).

Let us now consider several limiting cases and write the expressions for the average density \bar{n} for them.

Table 3: Numerical values of the quantities n_{gc} , $n_g^{(1)}$, as well as the roots $\sigma_{030}'^{(-)}$, $\sigma_{010}'^{(+)}$ of a specific cubic equation and the coefficients $\sigma_{00c}^{(-)}(\sigma_{030}'^{(-)})$, $\sigma_{00c}^{(-)}(\sigma_{010}'^{(+)})$ in Eqs. (30), (31).

n_{gc}	$n_g^{(1)}$	$\sigma_{030}'^{(-)}$	$\sigma_{010}'^{(+)}$	$\sigma_{00c}^{(-)}(\sigma_{030}'^{(-)})$	$\sigma_{00c}^{(-)}(\sigma_{010}'^{(+)})$
0.9971	-7.3776	-3.3745	3.3745	-0.8359	0.8359

4 Density for some limiting cases

The equation (9), taking into account the expression (21), takes the form

$$\bar{n} = n_{gc} + n_g^{(1)}\tau - M + \sigma_{00}^{(-)} \left(\tilde{h}^2 + h_{cm}^2 \right)^{\frac{d-2}{2(d+2)}}. \quad (23)$$

The general form of Eq. (23) naturally allows for the transition to cases where one of the variables (temperature or chemical potential) is the determining factor in describing the behavior of the order parameter.

Let us describe the behavior of \bar{n} for some limiting cases. One such case is the absence of chemical potential M ($M = 0$, and hence $\tilde{h} = 0$) while $T \neq T_c$. Then we have

$$\sigma_{00}^{(-)} \Big|_{M=0} = \left(1 + \frac{1}{2}\tau \right) \sigma_{00c}^{(-)}(\sigma_0'), \quad (24)$$

where

$$\sigma_{00c}^{(-)}(\sigma_0') = \frac{1}{(\beta_c W(0))^{1/2}} \left[e_0^{(-)} + \frac{f_{Iv}}{s^3} \right], \quad (25)$$

and $e_0^{(-)} = \sigma_0' s^{-1/2}$. The quantity σ_0' is a solution of a specific cubic equation (see Refs. [5, 19]). The form of the solutions of this equation depends on the sign of the discriminant. The renormalization group parameter s determines the division of the phase space of collective variables into layers [20, 21]. The expression for f_{Iv} is given in [5]. Based on Eq. (23), we obtain the dependence

$$\bar{n} = n_{gc} + n_g^{(1)}\tau + \sigma_{00}^{(-)} \Big|_{M=0} \tilde{\tau}_1^\beta. \quad (26)$$

Here the critical exponent $\beta = \nu/2$ is determined by the critical exponent of the correlation length ν ². The quantity $\tilde{\tau}_1$ is defined in Eq. (12).

Another limiting case is $M \neq 0$ and $T = T_c$ ($\tau = 0$, and hence $\tilde{\tau}_1 = 0$). According to Eq. (23), the density \bar{n} at $T = T_c$ satisfies the equality

$$\bar{n} = n_{gc} - M + \sigma_{00}^{(-)} \Big|_{T=T_c} \tilde{h}^{1/\delta}, \quad (27)$$

where

$$\sigma_{00}^{(-)} \Big|_{T=T_c} = \frac{6}{5} \frac{1}{(\beta_c W(0))^{1/2}} \left[e_0^{(-)} + \gamma_s^{(-)} - e_2^{(-)} \right], \quad (28)$$

and $\tilde{h} = M(\beta_c W(0))^{1/2}$, $\delta = (d+2)/(d-2)$. The quantity $e_2^{(-)}$, like $e_0^{(-)}$, depends on σ'_0 . The coefficient $\gamma_s^{(-)}$ characterizes the non-analytical contribution to the thermodynamic potential. The expressions for these quantities are given in Ref. [5].

In the general case ($M \neq 0$ and $T \neq T_c$), Eq. (23) can be rewritten as

$$\bar{n} = n_{gc} + n_g^{(1)}\tau - M + \sigma_{00}^{(-)} \left(\tilde{h}^2 + \tilde{\tau}_1^{2\beta\delta} \right)^{1/(2\delta)}. \quad (29)$$

Note that $M \ll 1$, and $\tilde{h} \sim M$. Therefore, the term M in the right-hand sides of Eqs. (23), (27), and (29) is significantly smaller than the last term and can be neglected.

5 Equation for the order parameter and the diameter of the coexistence curve

Let us proceed to deriving the equations that describe the binodal curve in a narrow temperature interval near the critical point. Numerical calculations will be illustrated by an example of the parameters of the Morse interaction potential, which are characteristic of sodium (Na) and are given in Section 3. Based on Eqs. (12), (24), and (26), we obtain the following formulas for the gas density \bar{n}_G and the liquid density \bar{n}_L :

$$\bar{n}_G = n_{gc} - n_g^{(1)}(-\tau) + \left(\frac{c_{11}}{q} E_2^{n_0} \right)^\beta \sigma_{00c}^{(-)} (\sigma'_{030}{}^{(-)}) (-\tau)^\beta \quad (30)$$

²It is conventional in physics to denote the inverse temperature by β , while the same symbol is also commonly used for the order parameter critical exponent. The intended meaning will be evident from the context.

and

$$\bar{n}_L = n_{gc} - n_g^{(1)}(-\tau) + \left(\frac{c_{11}}{q}E_2^{n_0}\right)^\beta \sigma_{00c}^{(-)}(\sigma_{010}'^{(+)})(-\tau)^\beta. \quad (31)$$

Note that $\tau < 0$ and $|\tau| \ll 1$. In the right-hand sides of Eqs. (30) and (31), we have neglected the term proportional to $(-\tau)^{\beta+1}$ since it is less significant than the term proportional to $(-\tau)^\beta$. The roots $\sigma_{030}'^{(-)}$ and $\sigma_{010}'^{(+)}$ of a specific cubic equation (see Ref. [19] and Table 3) refer to the chemical potentials $M = -0$ and $M = +0$, respectively. The coefficients $\sigma_{00c}^{(-)}(\sigma_{030}'^{(-)})$ and $\sigma_{00c}^{(-)}(\sigma_{010}'^{(+)})$ can be obtained from Eq. (25) by substituting the quantities $\sigma_{030}'^{(-)}$ and $\sigma_{010}'^{(+)}$, respectively, in place of σ_0' . For convenience, numerical values of the other coefficients appearing in Eqs. (30) and (31) are given in Table 4.

Table 4: The quantities c_{11} , q , E_2 , n_0 , and β appearing in Eqs. (30) and (31).

c_{11}	q	E_2	n_0	β
0.9425	1.2356	8.3079	0.5000	0.3024

Considering that $\sigma_{00c}^{(-)}(\sigma_{030}'^{(-)}) = -\sigma_{00c}^{(-)}(\sigma_{010}'^{(+)})$ (see Table 3) and using Eqs. (30) and (31), we arrive at the scaling equation

$$\frac{1}{2}(\bar{n}_L - \bar{n}_G) = B_0|\tau|^\beta. \quad (32)$$

Here

$$B_0 = \left(\frac{c_{11}}{q}E_2^{n_0}\right)^\beta \sigma_{00c}^{(-)}(\sigma_{010}'^{(+)}). \quad (33)$$

The order parameter of the studied continuous system is defined as

$$\frac{\bar{n}_L - \bar{n}_G}{n_{gc}} = \frac{2B_0}{n_{gc}}|\tau|^\beta. \quad (34)$$

The equation describing the law of rectilinear diameter of the liquid-gas co-existence curve has the form

$$\frac{\bar{n}_L + \bar{n}_G}{2} = n_{gc} + D_1|\tau|. \quad (35)$$

For the coefficient of the term linear in τ , we find

$$D_1 = -n_g^{(1)}. \quad (36)$$

The expression for $n_g^{(1)}$, as well as for n_{gc} , is presented in Section 3 [see Eqs. (22)]. The quantities B_0 and D_1 are given in Table 5.

Table 5: The coefficient B_0 in expression (34) for the order parameter and the coefficient D_1 in equation (35) for the rectilinear diameter.

B_0	D_1
1.0608	7.3776

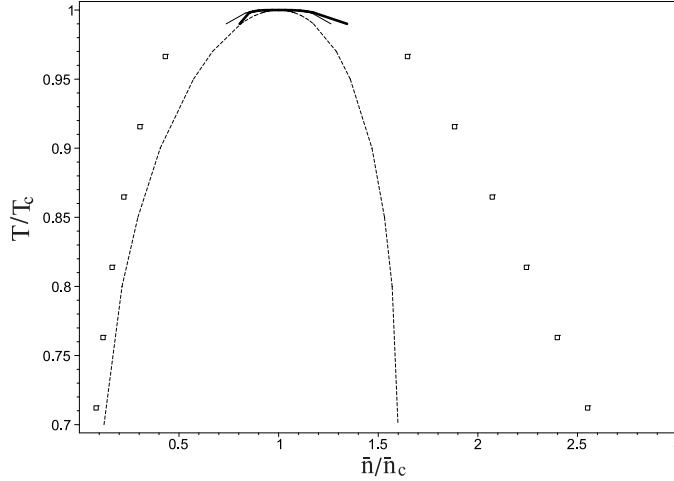


Figure 1: Upper part of the binodal for sodium in the temperature-density plane. The bold solid line represents the result of a calculation that includes an analytical temperature-dependent term. The thin solid line shows the result obtained without this term. The dashed line represents the zero-mode approximation [17]. Boxes indicate Monte Carlo simulation data [2].

It should be noted that the present approach is aimed at calculating and analyzing the characteristics of the system in a narrow vicinity of T_c ($|\tau| < \tau^* \sim 10^{-2}$, see [20, 21]), where theoretical and experimental research is difficult to carry out.

The upper part of the liquid-gas coexistence curve, obtained from Eqs. (30) and (31) for the parameters of the Morse interaction potential corresponding to sodium (Na), is shown in Fig. 1 as a bold solid line. This line corresponds to the case where the calculation of the relevant quantities, particularly the coefficients $a_n(T)$ from Eq. (17), includes the contribution from the analytical term proportional to τ (i.e., the linear temperature dependence). The thin solid line in Fig. 1 corresponds to the case where the analytical term is neglected in the calculation (in particular, the coefficients $a_n(T)$ are taken at $T = T_c$). For comparison, the coexistence curve obtained for Na within the so-called zero-mode approximation [17], which corresponds to the mean-field approximation, is also shown in the figure as a dashed line. The data obtained by Monte Carlo simulations [2] are shown as boxes.

Figure 1 shows which curve better agrees with the extrapolated data for Na, based on computer simulations [2] extended to $T/T_c \approx 1$. The zero-mode approximation (dashed line) does not account for order parameter fluctuations and is ineffective in the immediate vicinity of T_c . For the liquid branch of the binodal, better agreement is provided by the bold solid line (the case with analytical temperature-dependent term included). The gas branch of the binodal is better approximated (i.e., closer to the Monte Carlo results) by the thin solid line (the case where analytical temperature-dependent term is neglected).

The binodal curves from Fig. 1, along with their corresponding diameters, are shown in Fig. 2 in the immediate vicinity of the critical point. A finer scale is used along the ordinate axis compared to Fig. 1.

The upper parts of the binodals along with their corresponding diameters are shown separately in Figs. 3 and 4, for different methods of computing the gas branch of the binodal (see the respective figure captions for details). As noted above, the gas branch of the binodal in Fig. 4, compared to that in Fig. 3, provides a better reproduction of the Monte Carlo simulation results [2] extrapolated to the immediate vicinity of the critical point.

6 Conclusions

The present work has focused on the investigation of Morse fluid behavior near the critical point within the framework of a cell model. The vicinity of the critical point is of both fundamental and practical interest, while also being challenging to analyze due to the significant role of fluctuation effects.

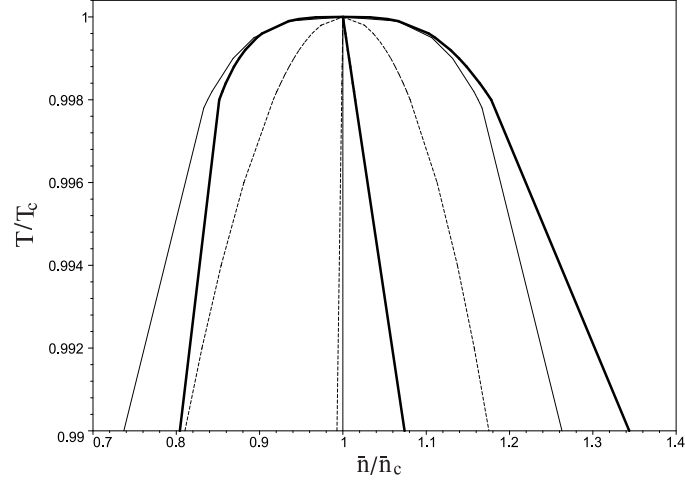


Figure 2: Liquid-gas coexistence curves and their diameters obtained in the immediate vicinity of the critical point using different calculation methods. Curve notations are the same as in Fig. 1.

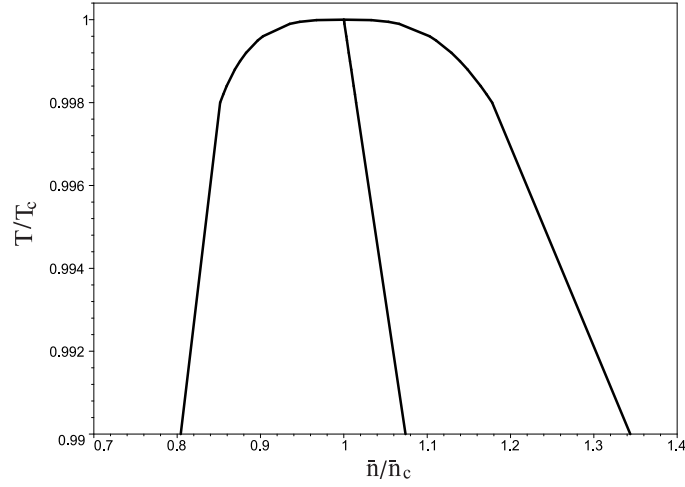


Figure 3: Upper part of the liquid-gas coexistence curve and its diameter, obtained with analytical temperature-dependent term included in both the liquid and gas branch calculations.

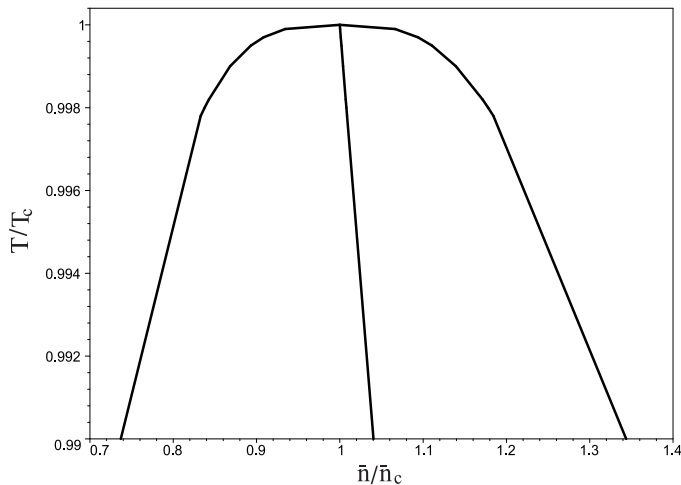


Figure 4: Upper part of the liquid-gas coexistence curve and its diameter, obtained with analytical temperature-dependent term included in the liquid branch calculation but omitted in the gas branch.

An analytical procedure has been developed for constructing the liquid-gas coexistence curve and calculating its diameter in the critical region. The numerical evaluation of the relevant quantities has been illustrated using Morse potential parameters typical for sodium. The critical point parameters for liquid alkali metals, sodium and potassium, previously obtained within our approach (see [4, 5, 17]), are consistent with available experimental data.

The analysis of the relationship between density and chemical potential at subcritical temperatures has enabled the derivation of equations describing the liquid-gas coexistence curve in the temperature-density plane. An explicit expression has been derived for the analytical temperature-dependent term appearing in the equation for the rectilinear diameter of the binodal. The upper part of the liquid-gas coexistence curve and its diameter have been constructed both with and without including the analytical temperature-dependent term in the calculation. A condition has been established that improves the agreement of the binodal branches with Monte Carlo simulation data [2] extrapolated to the immediate vicinity of the critical point. It has been clearly demonstrated that better agreement is achieved when the analytical temperature-dependent term is neglected in the calculation of the gas branch, but retained in the calculation of the liquid branch.

The analytical approach developed for a simple fluid system may prove

useful for investigating the critical behavior of multicomponent fluids. The present study also represents a certain methodological contribution to the theoretical description of critical phenomena.

Funding: This work was partly supported by the National Research Foundation of Ukraine under the project No. 2023.03/0201.

References

- [1] H. Okumura, F. Yonezawa, Liquid-vapor coexistence curves of several interatomic model potentials, J. Chem. Phys. 113 (2000) 9162-9168, <https://doi.org/10.1063/1.1320828>.
- [2] J.K. Singh, J. Adhikari, S.K. Kwak, Vapor-liquid phase coexistence curves for Morse fluids, Fluid Phase Equilib. 248 (2006) 1-6, <https://doi.org/10.1016/j.fluid.2006.07.010>.
- [3] E.M. Apfelbaum, The calculation of vapor-liquid coexistence curve of Morse fluid: Application to iron, J. Chem. Phys. 134 (2011) 194506, <https://doi.org/10.1063/1.3590201>.
- [4] M.P. Kozlovskii, I.V. Pylyuk, O.A. Dobush, The equation of state of a cell fluid model in the supercritical region, Condens. Matter Phys. 21 (2018) 43502, <https://doi.org/10.5488/CMP.21.43502>.
- [5] I.V. Pylyuk, Fluid critical behavior at liquid-gas phase transition: Analytic method for microscopic description, J. Mol. Liq. 310 (2020) 112933, <https://doi.org/10.1016/j.molliq.2020.112933>.
- [6] I.V. Pylyuk, M.P. Kozlovskii, O.A. Dobush, M.V. Dufanets, Morse fluids in the immediate vicinity of the critical point: Calculation of thermodynamic coefficients, J. Mol. Liq. 385 (2023) 122322, <https://doi.org/10.1016/j.molliq.2023.122322>.
- [7] O.A. Dobush, M.P. Kozlovskii, R.V. Romanik, I.V. Pylyuk, Thermodynamic response functions in a cell fluid model, Ukr. J. Phys. 69 (2024) 919-929, <https://doi.org/10.15407/ujpe69.12.919>.
- [8] J.F. Nicoll, Critical phenomena of fluids: Asymmetric Landau-Ginzburg-Wilson model, Phys. Rev. A 24 (1981) 2203-2220, <https://doi.org/10.1103/PhysRevA.24.2203>.

- [9] S. Jüingst, B. Knuth, F. Hensel, Observation of singular diameters in the coexistence curves of metals, *Phys. Rev. Lett.* 55 (1985) 2160-2163, <https://doi.org/10.1103/PhysRevLett.55.2160>.
- [10] V.L. Kulinskii, N.P. Malomuzh, The nature of the rectilinear diameter singularity, *Physica A* 388 (2009) 621-627, <https://doi.org/10.1016/j.physa.2008.11.014>.
- [11] S.C. Greer, B.K. Das, A. Kumar, E.S.R. Gopal, Critical behavior of the diameters of liquid-liquid coexistence curves, *J. Chem. Phys.* 79 (1983) 4545-4552, <https://doi.org/10.1063/1.446369>.
- [12] Y. Garrabos, C. Lecoutre, S. Marre, D. Beysens, I. Hahn, Liquid-vapor rectilinear diameter revisited, *Phys. Rev. E* 97 (2018) 020101, <https://doi.org/10.1103/PhysRevE.97.020101>.
- [13] O. Bakai, M. Bratchenko, S. Dyuldy, On the singularity of the liquid-gas coexistence curve diameter, *Ukr. J. Phys.* 65 (2020) 802-809, <https://doi.org/10.15407/ujpe65.9.802>.
- [14] A.V. Tatarenko, Coexistence curve diameter and slope of vapor pressure: “universal” relation in the critical region, *J. Mol. Liq.* 394 (2024) 123776, <https://doi.org/10.1016/j.molliq.2023.123776>.
- [15] A.L. Rebenko, Cell gas model of classical statistical systems, *Rev. Math. Phys.* 25 (2013) 1330006, <https://doi.org/10.1142/S0129055X13300069>.
- [16] V.A. Boluh, A.L. Rebenko. Cell gas free energy as an approximation of the continuous model, *J. Mod. Phys.* 6 (2015) 168-175, <https://doi.org/10.4236/jmp.2015.62022>.
- [17] M.P. Kozlovskii, O.A. Dobush, I.V. Pylyuk, Using a cell fluid model for the description of a phase transition in simple liquid alkali metals, *Ukr. J. Phys.* 62 (2017) 865-873, <https://doi.org/10.15407/ujpe62.10.0865>.
- [18] R.C. Lincoln, K.M. Koliwad, P.B. Ghate, Morse-potential evaluation of second- and third-order elastic constants of some cubic metals, *Phys. Rev.* 157 (1967) 463-466, <https://doi.org/10.1103/PhysRev.157.463>.

- [19] I.V. Pylyuk, M.P. Kozlovskii, First-order phase transition in the framework of the cell fluid model: Regions of chemical potential variation and the corresponding densities, Ukr. J. Phys. 67 (2022) 54-61, <https://doi.org/10.15407/ujpe67.1.54>.
- [20] I.R. Yukhnovskii, Phase Transitions of the Second Order. Collective Variables Method, World Scientific, Singapore, 1987.
- [21] I.R. Yukhnovskii, M.P. Kozlovskii, I.V. Pylyuk, Microscopic Theory of Phase Transitions in the Three-Dimensional Systems, Eurosvit, Lviv, 2001 [in Ukrainian].